論文 / 著書情報
Article / Book Information

論題(和文)	
Title(English)	Spectral characteristics of a 1.3-μm npn-AlGaInAs/InP transistor laser under various operating conditions
著者(和文)	行成 元志, 佐藤 憲明, 西山 伸彦, 荒井 滋久
Authors(English)	Masashi Yukinari, Noriaki Sato, Nobuhiko Nishiyama, Shigehisa Arai
出典(和文)	, Vol. 11, No. 18, pp. 1-6
Citation(English)	IEICE Electronics Express, Vol. 11, No. 18, pp. 1-6
発行日 / Pub. date	2014, 8
URL	http://search.ieice.org/
権利情報 / Copyright	本著作物の著作権は電子情報通信学会に帰属します。 Copyright (c) 2014 Institute of Electronics, Information and Communication Engineers.

ELectronics EXpress

LETTER

IEICE Electronics Express, Vol.11, No.18, 1–6

Spectral characteristics of a 1.3-µm npn-AlGaInAs/InP transistor laser under various operating conditions

Masashi Yukinari[1], **Noriaki Sato**[1], **Nobuhiko Nishiyama**[1a)], **and Shigehisa Arai**[1,2]

[1] *Department of Electrical and Electronic Engineering, Tokyo Institute of Technology, 2–12–1 O-okayama, Meguro-ku, Tokyo 152–8552, Japan*

[2] *Quantum Nanoelectronics Research Center, Tokyo Institute of Technology, 2–12–1 O-okayama, Meguro-ku, Tokyo 152–8552, Japan*

a) *n-nishi@pe.titech.ac.jp*

Abstract: The spectral characteristics of a 1.3-µm npn-AlGaInAs/InP transistor laser were studied under various collector–base voltages and emitter currents. The result shows that the peak wavelength shifts as a function of the output power resulting from voltage and current controls exhibited contrasting behavior under a continuous-wave operation.

Keywords: semiconductor laser, transistor laser, AlGaInAs/InP

Classification: Optoelectronics, Lasers and quantum electronics, Ultrafast optics, Silicon photonics, Planar lightwave circuits

References

[1] A. Tomita and A. Suzuki: IEEE J. Quantum Electron. **23** (1987) 1155. DOI:10.1109/JQE.1987.1073481

[2] U. Menzel, A. Bärwolff, P. Enders, D. Ackermann, R. Puchert and M. Voss: Semicond. Sci. Technol. **10** (1995) 1382. DOI:10.1088/0268-1242/10/10/013

[3] N. Iwai, M. Wakaba, M. Kobayakawa, K. Kiyota, T. Kurobe, G. Kobayashi, T. Kimoto, S. Tamura, T. Mukaihara, N. Yokouchi, H. Ishii and A. Kasukawa: The 23rd IEEE International Semiconductor Laser Conference (2012) TuA2. DOI:10.1109/ISLC.2012.6348323

[4] J. Shibata, Y. Mori, Y. Sasai, N. Hase, H. Serizawa and T. Kajiwara: Electron. Lett. **21** (1985). DOI:10.1049/el:19850068

[5] R. Chan, M. Feng, N. Holonyak and G. Walter: Appl. Phys. Lett. **86** (2005) 131114. DOI:10.1063/1.1889243

[6] B. Faraji, S. Wei, D. L. Pulfrey and L. Chrostowski: IEEE J. Sel. Top. Quantum Electron. **15** (2009) 594. DOI:10.1109/JSTQE.2009.2013178

[7] G. Walter, C. H. Wu, H. W. Then, M. Feng and N. Holonyak, Jr.: Appl. Phys. Lett. **94** (2009) 241101. DOI:10.1063/1.3153146

[8] M. Shirao, S. Lee, N. Nishiyama and S. Arai: IEEE J. Quantum Electron. **47** (2011) 359. DOI:10.1109/JQE.2010.2090341

[9] I. Taghavi, H. Kaatuzian and J. P. Leburton: Appl. Phys. Lett. **100** (2012) 231114. DOI:10.1063/1.4727898

[10] M. Shirao, N. Nishiyama, N. Sato and S. Arai: IEICE Electron. Express **9** (2012) 1792. DOI:10.1587/elex.9.1792

DOI: 10.1587/elex.11.20140679
Received July 16, 2014
Accepted August 4, 2014
Publicized August 25, 2014
Copyedited September 25, 2014

IEICE Electronics Express, Vol.11, No.18, 1–6

[11] M. Feng, N. Holonyak, A. James, K. Cimino, G. Walter and R. Chan: Appl. Phys. Lett. **89** (2006) 113504. DOI:10.1063/1.2346369
[12] M. Feng, N. Holonyak, H. W. Then and G. Walter: Appl. Phys. Lett. **91** (2007) 053501. DOI:10.1063/1.2767172
[13] R. Basu, B. Mukhopadhyay and P. K. Basu: IEEE Photon. J. **4** (2012) 1572. DOI:10.1109/JPHOT.2012.2211075
[14] M. Shirao, T. Sato, Y. Takino, N. Sato, N. Nishiyama and S. Arai: The 23rd International Conference on Indium Phosphide and Related Materials (2011) P5.60.
[15] N. Sato, M. Shirao, T. Sato, M. Yukinari, N. Nishiyama, T. Amemiya and S. Arai: IEEE J. Select. Top. Quantum Electron. **19** (2013) 1502608. DOI:10.1109/JSTQE.2013.2250490
[16] Y. Takino, M. Shirao, N. Sato, T. Amemiya, N. Nishiyama and S. Arai: J. Quantum Electron **48** (2012) 971. DOI:10.1109/JQE.2012.2196410
[17] D. A. B. Miller, D. S. Chemla and S. Schmitt-Rink: Phys. Rev. B **33** (1986) 6976. DOI:10.1103/PhysRevB.33.6976

1 Introduction

In optical fiber communications, especially for WDM transmission, wavelength stabilization of the light source while controlling the output power is the most critical point. In conventional laser diodes (LDs), output power control can be realized by changing the injection current; however, this process causes a wavelength shift because of Joule heating [1, 2]. As a result, conventional LDs cannot control the output power while maintaining the wavelength. Therefore, for such applications, recent light sources such as tunable lasers have integrated semiconductor optical amplifiers to independently control the output power [3]. In contrast, another approach is to install built-in output power control function with no Joule heating in the LD itself. One of the candidates for such function is the transistor laser (TL), which is based on a heterojunction bipolar transistor with an active layer at its base region [4]. Owing to its three-terminal structure, the TL can achieve output power control with different spectral characteristics compared with conventional lasers by applying a collector–base voltage. In addition, the TL has the potential to break the modulation speed limitations inherent in conventional LDs because shorter carrier recovery times can be achieved [5, 6, 7, 8, 9, 10]. Until now, several studies on the 0.98-µm TLs have been have been conducted [11, 12, 13]. In our previous reports, we successfully achieved the first room-temperature continuous-wave (RT-CW) operation at longer wavelengths as well as the transistor characterization of a pnp [14] and an npn TL emitting at the 1.3-µm wavelength using an AlGaInAs/InP material system [15].

In the present paper, we will report the study on the spectral characteristics of 1.3-µm npn-AlGaInAs/InP TLs under various collector–base voltages. Comparison with those under various emitter currents is also presented.

2 Device structure

The schematic structure of the fabricated npn-TL in this study is shown in Fig. 1. The initial wafer was grown on a (100) n-InP substrate using an organo-metallic

DOI: 10.1587/elex.11.20140679
Received July 16, 2014
Accepted August 4, 2014
Publicized August 25, 2014
Copyedited September 25, 2014

vapor phase epitaxy technique. The initial wafer consisted of an n-AlGaInAs emitter, five fully strain-compensated AlGaInAs quantum wells [(QWs) with $\lambda_g = 1.3$-µm, 5-nm-thick well, and 10-nm-thick barrier], a p-AlGaInAs (with $\lambda_g = 1.07\,\mu m$ and 80-nm thick), and a p-GaInAsP (with $\lambda_g = 1.17\,\mu m$ and 30-nm thick). Although we intentionally did not dope the QWs, Zn diffusion was confirmed to make a p-type transistor base. A buried hetero (BH) structure with n/p/n/p-InP current-blocking layers was formed by wet etching and selective regrowth [15]. After the BH structure formation, a 200-nm-thick p-GaInAsP base layer ($E_g = 1.06\,eV$; $N_A = 1 \times 10^{18}\,cm^{-3}$), an n-InP collector layer (2000-nm thick), an n^+-GaInAs collector contact layer, (50-nm thick; $N_D = 1 \times 10^{19}\,cm^{-3}$), and a p^+-GaInAs base contact layer (50-nm thick; $N_A = 1 \times 10^{19}\,cm^{-3}$) were formed at the side through several regrowth steps. The collector and base mesas were formed using RIE and wet etching. Finally, the collector, base, and emitter (backside) electrodes were formed by evaporating Ti/Au (25 nm/200 nm) onto the device. The details of the fabrication process can be found in our previous reports [15, 16]. Laser cavities were formed by cleavage with no high-reflection coating.

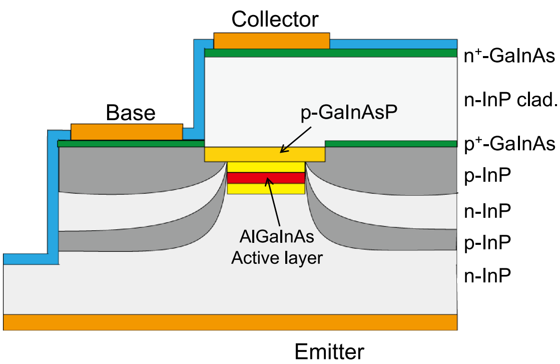

Fig. 1. Structure of an npn-AlGaInAs/InP TL.

3 Measurement

Fig. 2 shows the current–output power (*I–L*) characteristics of the TL with a common–base (CB) configuration under a CW condition at a stage temperature of 10 °C. The cavity length and the stripe width were 1000 and 1.5 µm, respectively. A threshold emitter current of 40 mA (current density $J_{th} = 2.7\,kA/cm^2$) and a differential quantum efficiency of 7% from both facets were obtained. By applying collector–base voltage V_{CB}, both an increase in the threshold current and a decrease in the output power were observed because of the optical absorption at the p-GaInAsP base layer due to the Franz–Keldysh and the Early effects, which increased the collector current. Thus, a higher emitter current was needed to boost the base current to reach the threshold [17].

Therefore, the output power can be controlled by controlling V_{CB} without changing the emitter current, which changes the amount of Joule heating. The TLs used in the current study had a very small electrical amplification ($\beta < 1$; therefore, the devices used in the experiment were not actually "transistors" in terms of electrical characteristics although they have "transistor" structures) by having a

DOI: 10.1587/elex.11.20140679
Received July 16, 2014
Accepted August 4, 2014
Publicized August 25, 2014
Copyedited September 25, 2014

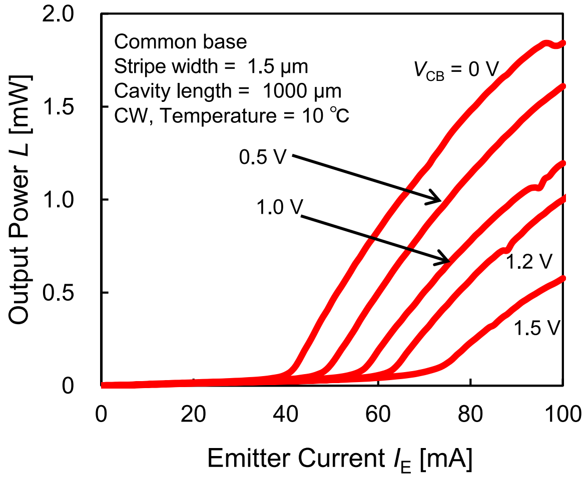

Fig. 2. Lasing characteristics under a CB configuration.

relatively thick p-GaInAsP base layer for the purpose of output power control without changing the amount of Joule heating. Using this device, the lasing spectra were measured by varying both emitter current I_E and V_{CB}. Because the device had a FP cavity structure and showed a multi-longitudinal-mode operation, we traced one peak mode.

Figs. 3 and 4 show the lasing wavelength as a function of I_E with various V_{CB} values under CW and pulsed operations (pulse width = 1 μs and repetition = 1 kHz), respectively. Under the CW operation (Fig. 3), the peak lasing wavelength was red shifted by increasing I_E because of the Joule heating, which is the same as that of conventional LDs. On the other hand, under the pulsed operation (Fig. 4), no wavelength shift was observed by increasing I_E, whereas a slight red shift was observed by increasing V_{CB}, which may be attributed to either the refractive-index change or large quantum-confined Stark effect (QCSE), as discussed later.

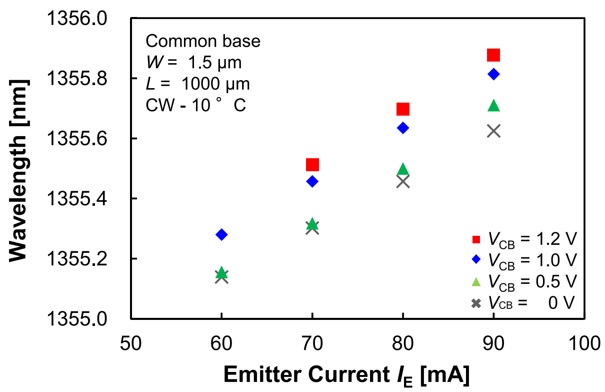

Fig. 3. Lasing wavelength as a function of I_E under CW operation.

Next, the lasing wavelength as a function of V_{CB} with various emitter currents was measured under CW and pulsed operations, as shown in Figs. 5 and 6, respectively. Fig. 5 shows that a red shift was observed by increasing I_E under the CW operation because of the Joule heating, as mentioned before. The peak lasing wavelength of the TL was red shifted as V_{CB} was increased even under the pulsed operation, which means that the shift was not caused by Joule heating.

DOI: 10.1587/elex.11.20140679
Received July 16, 2014
Accepted August 4, 2014
Publicized August 25, 2014
Copyedited September 25, 2014

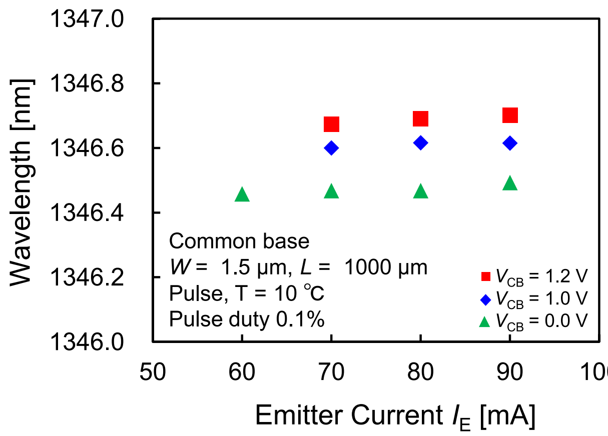

Fig. 4. Lasing wavelength as a function of I_E under pulse operation.

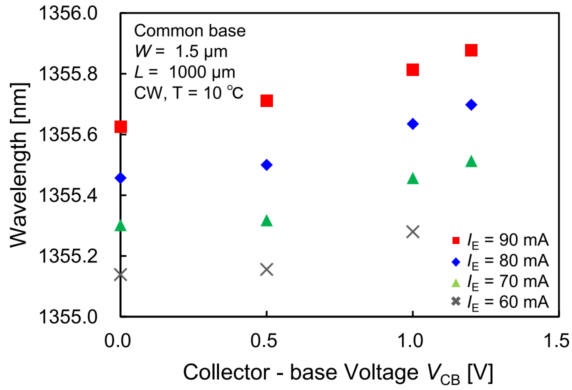

Fig. 5. Lasing wavelength as a function of collector–base voltage under CW operation.

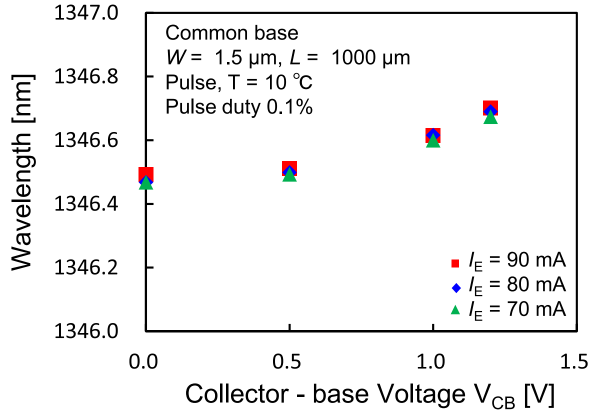

Fig. 6. Lasing wavelength as a function of collector–base voltage under pulse operation.

Although the reason for this phenomenon is still under investigation, this phenomenon could be considered as either a refractive-index change in the p-GaInAsP by V_{CB} or a large QCSE in the QW active region that exceeds the amount of carrier screening effect.

Finally, Fig. 7 shows the peak lasing wavelength as a function of the output power under the CW operation. The red squares indicate the output power

DOI: 10.1587/elex.11.20140679
Received July 16, 2014
Accepted August 4, 2014
Publicized August 25, 2014
Copyedited September 25, 2014

IEICE Electronics Express, Vol.11, No.18, 1–6

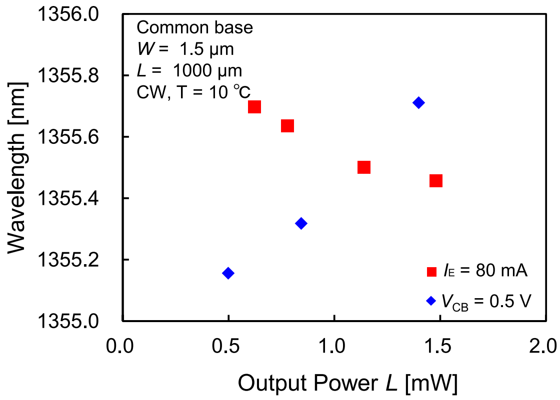

Fig. 7. Lasing wavelength as a function of the output power under CW operation. The blue diamonds show the characteristics under output power control by I_E with fixed V_{CB}. The red squares show the characteristics under output power control by V_{CB} with fixed I_E.

controlled by V_{CB} with a fixed I_{E} of 80 mA. The blue diamonds indicate the output power controlled by I_{E} with a fixed V_{CB} of 0.5 V. A difference between the two measurements is evident. When the output power was increased by I_{E}, the temperature rise in the device caused a red shift, as mentioned earlier. On the contrary, the lasing wavelength of the TL was blue shifted when the output power was increased by V_{CB}.

From this result, the combination of V_{CB} and I_{E} controls can achieve output power control without any wavelength change. We are currently investigating a structure that achieves no-wavelength-shift output power control by voltage modulation only.

4 Conclusion

In this study, we experimentally investigated the lasing wavelength behavior of a 1.3-μm npn-AlGaInAs/InP TL by varying the collector–base voltage and emitter current. The results showed contrasting wavelength-shift behavior between these two operating conditions under a CW operation and revealed that output power control by the collector–base voltage can be possible without Joule heating in the TL that uses this material system.

Acknowledgments

This work was supported in part by the JSPS KAKENHI Grants (#24246061, #22360138, and #21226010) from the Ministry of Education, Culture, Sports, Science and Technology, Japan (MEXT).

DOI: 10.1587/elex.11.20140679
Received July 16, 2014
Accepted August 4, 2014
Publicized August 25, 2014
Copyedited September 25, 2014